

A line search framework with restarting for noisy optimization problems

Albert S. Berahas ^{*} Michael J. O’Neill [†] Clément W. Royer [‡]

October 21, 2025

Abstract

Nonlinear optimization methods are typically iterative and make use of gradient information to determine a direction of improvement and function information to effectively check for progress. When this information is corrupted by noise, designing a convergent and practical algorithmic process becomes challenging, as care must be taken to avoid taking bad steps due to erroneous information. For this reason, simple gradient-based schemes have been quite popular, despite being outperformed by more advanced techniques in the noiseless setting. In this paper, we propose a general algorithmic framework based on line search that is endowed with iteration and evaluation complexity guarantees even in a noisy setting. These guarantees are obtained as a result of a restarting condition, that monitors desirable properties for the steps taken at each iteration and can be checked even in the presence of noise. Experiments using a nonlinear conjugate gradient variant and a quasi-Newton variant illustrate that restarting can be performed without compromising practical efficiency and robustness.

1 Introduction

Gradient descent techniques are iterative, simple, require only first-order (gradient) information, and have emerged as some of the most versatile algorithms for smooth nonlinear optimization. In particular, their application in the presence of noise has received significant attention from the optimization and machine learning communities [5]. Under appropriate assumptions on the noise, complexity guarantees can be derived for gradient-type methods, even when those techniques use a line search in lieu of fixed or predetermined step size sequences [3, 24]. That said, there exist numerous advanced optimization routines that are known to outperform gradient descent in practice for noiseless problems, such as quasi-Newton and nonlinear conjugate gradient methods [27]. These algorithms are notoriously difficult to endow with complexity guarantees in the nonconvex (or sometimes even convex) setting. In fact, it is unclear whether those methods can exhibit better theoretical guarantees than simple gradient descent schemes, in a way that

^{*}Department of Industrial & Operations Engineering, University of Michigan, Ann Arbor, MI 48109-2102, USA (albertberahas@gmail.com).

[†]Department of Statistics and Operations Research, University of North Carolina at Chapel Hill, Chapel Hill, NC 27514, USA (mikeoneill@unc.edu).

[‡]LAMSADE, CNRS, Université Paris Dauphine-PSL, 75016 Paris, France (clement.royer@lamsade.dauphine.fr).

matches their practical performance. The situation is even more complicated in settings where the function and gradient information these procedures rely upon to generate and validate search directions is corrupted with noise.

In spite of these challenges, complexity results have recently been obtained by considering problems for which access to function and gradient information is corrupted with noise of a known or estimable level. Problems of this type naturally arise in numerous fields such as machine learning [15, 16], black-box optimization [1, 13, 25], and simulation optimization [29, 30]. Several algorithms based on globalization techniques (e.g., line/step search, trust-region) and quasi-Newton updates have been proposed in recent years to tackle this class of problems [2, 4, 23, 34, 31]. In a parallel line of work, various algorithmic strategies have been developed for the regime where the gradient estimates are sufficiently accurate with reasonable probability [3, 11, 24, 28, 7, 32]. While complexity results are available for all of the aforementioned methods, almost all of them are based on simple, gradient descent-type steps.

In this work, we propose a general algorithmic framework of line search type for the unconstrained minimization of noisy functions endowed with worst-case complexity guarantees. We build upon the restarting conditions developed for deterministic nonlinear conjugate gradient methods by Chan–Renous–Legoubin and Royer [12] and prove that these conditions remain sufficient for establishing worst-case complexity results even in the presence of noise, under a noise condition that is on par with existing literature. Our algorithmic framework adaptively chooses the step size at each iteration via a robust line search procedure that uses the estimated noise level present in function evaluations. We do not place restrictions on how search directions are generated in our framework, enabling it to be used in conjunction with a wide range of popular nonlinear optimization procedures including quasi-Newton and nonlinear conjugate gradient.

The paper is organized as follows. We describe our problem setting and algorithmic framework based on restarts in Section 2. We then derive complexity results for our framework in Section 3, where we also formalize our assumptions regarding the noise. In Section 4, we demonstrate the effectiveness of our approach numerically by comparing implementations of our framework based on quasi-Newton and nonlinear conjugate gradient methods. Finally, we provide some concluding remarks in Section 5.

2 Problem and algorithm

This paper focuses on the problem

$$\min_{x \in \mathbb{R}^n} \phi(x), \tag{2.1}$$

where $\phi : \mathbb{R}^n \rightarrow \mathbb{R}$ is a nonconvex, continuously differentiable function. In our setting, the objective function and its associated derivatives cannot be computed exactly. Instead, approximations that are contaminated with noise are available. We denote the function and gradient approximations of ϕ as f and g , respectively. The precise conditions on the quality of these approximations are stated in Section 3. Given a tolerance $\epsilon \in (0, 1)$, our goal is to compute an ϵ -approximate stationary point, that is, a vector $x \in \mathbb{R}^n$ such that

$$\|\nabla\phi(x)\| \leq \epsilon, \tag{2.2}$$

where $\|\cdot\|$ denotes the Euclidean norm in \mathbb{R}^n .

In this section, we extend the nonlinear CG method proposed by Chan–Renous–Legoubin and Royer [12] to allow for inexact function and gradient values and describe a nonlinear conjugate gradient method based on Armijo line search and a modified restart condition.

2.1 Algorithmic framework

Our proposed algorithmic framework is given in Algorithm 1. At every iteration, we perform a backtracking line search to compute a step that yields a suitable decrease in the objective function (see condition (2.3)). Note that this sufficient decrease condition (2.3) is relaxed by a parameter ϵ_f in order to account for potential noise in the objective function evaluations. This parameter is explicitly defined in Assumption 3.3.

Algorithm 1 Line search framework with restart conditions and noisy estimates

Inputs: $x_0 \in \mathbb{R}^d$, $\eta \in (0, \frac{1}{2}]$, $\rho \in (0, 1)$, $\sigma_d \in (0, 1]$, $\kappa_d \geq 1$, $p \geq 0$, $\epsilon_f \geq 0$.

- 1: Compute an estimate g_0 of $\nabla\phi(x_0)$.
- 2: Set $d_0 = -g_0$ and $k = 0$.
- 3: **for** $k = 0, 1, 2, \dots$ **do**
- 4: Compute $\alpha_k = \rho^{j_k}$ where j_k is the smallest nonnegative integer such that

$$f(x_k + \alpha_k d_k) < f(x_k) + \eta \alpha_k g_k^T d_k + 2\epsilon_f. \quad (2.3)$$

where $f(x_k + \alpha_k d_k)$ and $f(x_k)$ are estimates of $\phi(x_k + \alpha_k d_k)$ and $\phi(x_k)$, respectively.

- 5: Set $x_{k+1} = x_k + \alpha_k d_k$ and compute an estimate g_{k+1} of the gradient $\nabla\phi(x_{k+1})$.
- 6: Define a direction d_{k+1} using g_{k+1} .
- 7: If the condition

$$g_{k+1}^T d_{k+1} \geq -\sigma_d \|g_{k+1}\|^{1+p} \quad \text{or} \quad \|d_{k+1}\| \geq \kappa_d \|g_{k+1}\|^{\frac{1+p}{2}}, \quad (2.4)$$

holds, restart the algorithm by setting $d_{k+1} = -g_{k+1}$.

- 8: **end for**
-

Once the new point has been computed, we estimate the gradient at the new iterate, then use that estimate to compute a new search direction. The key ingredient in Algorithm 1 is the restarting condition (2.4), that determines whether the search direction (e.g., a nonlinear CG direction or a quasi-Newton direction) is kept for the next iteration. For any $k \geq 1$, if iteration $k - 1$ does not end with a restart, it follows that¹

$$g_k^T d_k \leq -\sigma_d \|g_k\|^{1+p} \quad \text{and} \quad \|d_k\| \leq \kappa_d \|g_k\|^{\frac{1+p}{2}}, \quad (2.5)$$

a condition more general than that commonly used in gradient-type methods for both deterministic and stochastic optimization [3, 10, 11, 19]. In this paper, we use $\frac{1+p}{2}$ in the second part of (2.5) rather than introducing an additional parameter. In addition to simplifying the notation, this condition was shown to be beneficial in terms of line search iterations in the deterministic setting [12].

On the other hand, if iteration $k - 1$ ends with a restart (2.4), it follows that $d_k = -g_k$, in which case (2.5) is satisfied with $p = \kappa_d = \sigma_d = 1$. More generally, when $p = 1$, condition (2.5)

¹Although the inequalities should be strict, we use non-strict inequalities for notational convenience.

becomes

$$g_k^\top d_k \leq -\sigma_d \|g_k\|^2 \quad \text{and} \quad \|d_k\| \leq \kappa_d \|g_k\|. \quad (2.6)$$

Such a condition is typical of gradient-related directions, and has been instrumental in obtaining complexity guarantees for gradient-type methods in the noiseless setting [10, 12]. In the context of nonlinear conjugate gradient methods, similar properties have been used to establish global convergence [20].

2.2 Algorithmic instances

The framework described in Algorithm 1 is quite generic, and covers a number of search direction choices. In our experiments, we will focus on two variants corresponding to classical nonlinear optimization methods.

Nonlinear conjugate gradient Nonlinear conjugate gradient (CG) methods set $d_0 = -g_0$ and $d_{k+1} = -g_{k+1} + \beta_{k+1}d_k$, where β_{k+1} is a conjugate parameter [21]. These methods can be classified as momentum-based methods, in that they combine current gradient information with the previously obtained search direction [33].

Quasi-Newton methods Quasi-Newton algorithms set $d_k = -H_k g_k$, where H_k is a symmetric positive definite approximation of the Hessian matrix. Quasi-Newton methods such as (L-)BFGS typically include a restart condition to avoid updates that would lead to indefiniteness of H_{k+1} [27, Chapter 6]. More precisely, the update is skipped (i.e. $H_{k+1} = H_k$) if

$$s_k^\top (g_{k+1} - g_k) \geq \tau \|s_k\| \|g_{k+1} - g_k\|, \quad (2.7)$$

fails, where $s_k = \alpha_k d_k = x_{k+1} - x_k$ and $\tau \in (0, 1)$. This process guarantees that $H_{k+1} \succ 0$. Interestingly, when (2.7) holds, we also have

$$g_{k+1}^\top (-H_{k+1} g_{k+1}) \leq -\lambda_{\min}(H_{k+1}) \|g_{k+1}\|^2 \quad \text{and} \quad \|H_{k+1} g_{k+1}\| \leq \lambda_{\max}(H_{k+1}) \|g_{k+1}\|,$$

and those conditions resemble (2.6) with $p = 1$.

3 Complexity analysis

In this section, we derive a complexity result for our line search framework with restart conditions and noisy estimates. Section 3.1 provides the necessary assumptions as well as intermediate results, while Section 3.2 establishes and discusses the complexity bound for our algorithm.

3.1 Assumptions and decrease guarantees

We make the following assumptions about the objective function of problem (2.1).

Assumption 3.1 *The function ϕ is continuously differentiable on \mathbb{R}^n and its gradient is L -Lipschitz continuous for $L > 0$.*

Assumption 3.2 *There exists $\phi_{\text{low}} \in \mathbb{R}$ such that $\phi(x) \geq \phi_{\text{low}}$ for every $x \in \mathbb{R}^n$.*

We now state an assumption regarding the objective function estimates, that involves the parameter ϵ_f used in Algorithm 1.

Assumption 3.3 *There exists a constant $\epsilon_f \geq 0$ such that for all $x \in \mathbb{R}^n$ the objective function estimate $f(x)$ of $\phi(x)$*

$$|f(x) - \phi(x)| \leq \epsilon_f. \quad (3.1)$$

The next assumption pertains to the objective function gradient estimates. This assumption is only required to hold for the iterates generated by Algorithm 1.

Assumption 3.4 *There exist constants $\sigma_\phi \in [0, 1)$ and $\epsilon_g \geq 0$ such that for all $k \in \mathbb{N}$ the objective gradient estimate at iteration k (denoted by g_k) satisfies*

$$\|g_k - \nabla\phi(x_k)\| \leq \max \left\{ \epsilon_g, \sigma_\phi \theta_p \min \left[\|\nabla\phi(x_k)\|, \|\nabla\phi(x_k)\|^{\frac{1+p}{2}} \right] \right\} \quad (3.2)$$

where $x_k \in \mathbb{R}^n$ are the iterates generated by Algorithm 1, $p \geq 0$ is the value used in (2.4), and θ_p is defined as

$$\theta_p := \frac{(1 - \eta)\sigma_d(1 - \sigma_\phi)^{1+p}}{2\kappa_d(1 + \sigma_\phi)^{\frac{1+p}{2}}}. \quad (3.3)$$

Assumption 3.4 resembles conditions previously used in the literature in that it generalizes norm conditions [9] as well as bounded noise [2]. Although we consider the true gradient on the right-hand side of condition (3.2), we point out that the gradient estimate could also be used, akin to [3, 6, 11]. Note that when $p = 1$, condition (3.2) becomes

$$\|g_k - \nabla\phi(x_k)\| \leq \max \{ \epsilon_g, \sigma_\phi \theta_p \|\nabla\phi(x_k)\| \}.$$

When $\sigma_\phi = 0$, condition (3.2) corresponds to bounded noise in the gradient estimates. Conversely, when $\epsilon_g = 0$, the condition becomes a norm condition involving the true gradient norm as well as a constant coefficient [9]. We note that some conditions proposed in the literature involve $\alpha_k \|g_k\|$ on the right-hand side rather than a constant times $\|\nabla\phi(x_k)\|$ [3]. We focus on using the true gradient norm $\|\nabla\phi(x_k)\|$ for simplicity in this paper, but we use a fixed quantity θ_p in lieu of the classical iteration-dependent quantity α_k . The former (θ_p) is sufficient to derive a lower bound on the step size, which typically exists for line search schemes. Using θ_p , which is associated with our worst-case lower-bound on α_k , instead of α_k may represent a stronger condition on some iterations. However, for sufficiently small α_k , this may not be the case, as θ_p is *independent* of the Lipschitz constant L , while any worst-case lower bound on α_k will be dependent on this quantity.

More broadly, our focus in this paper is to examine the effect of the restarting conditions in the noisy setting, and thus we focused on a single noise condition for that purpose. As we will see below, the use of $\|\nabla\phi(x_k)\|^{\frac{1+p}{2}}$ combined with (2.5) is instrumental for deriving complexity results. Those results are a generalization of the noiseless setting [12], that can be recovered for $\epsilon_f = \epsilon_g = 0$.

Lemma 3.1 *Let Assumption 3.4 hold, and suppose that at the k th iteration of Algorithm 1*

$$\min \left\{ \|\nabla\phi(x_k)\|, \|\nabla\phi(x_k)\|^{\frac{1+p}{2}} \right\} \geq \frac{\epsilon_g}{\sigma_\phi \theta_p}, \quad (3.4)$$

where θ_p is defined in (3.3). Then,

$$\|g_k\| \geq (1 - \sigma_\phi) \|\nabla\phi(x_k)\| \quad (3.5)$$

and

$$\|g_k\| \leq (1 + \sigma_\phi) \|\nabla\phi(x_k)\|. \quad (3.6)$$

Proof. We begin by proving (3.5). By Assumption 3.4, we have

$$\begin{aligned} \|\nabla\phi(x_k)\| &\leq \|\nabla\phi(x_k) - g_k\| + \|g_k\| \\ &\leq \max \left\{ \epsilon_g, \sigma_\phi \theta_p \min \left\{ \|\nabla\phi(x_k)\|, \|\nabla\phi(x_k)\| \frac{1+p}{2} \right\} \right\} + \|g_k\| \\ &\leq \sigma_\phi \theta_p \min \left\{ \|\nabla\phi(x_k)\|, \|\nabla\phi(x_k)\| \frac{1+p}{2} \right\} + \|g_k\| \\ &\leq \sigma_\phi \|\nabla\phi(x_k)\| + \|g_k\|, \end{aligned} \quad (3.7)$$

where the third inequality follows from (3.4) and the last inequality uses $\theta_p \leq 1$ (which follows from the definition (3.3) along with $\eta \in (0, \frac{1}{2}]$, $\sigma_\phi \in [0, 1)$, $\sigma_d \in (0, 1]$ and $\kappa_d \geq 1$). Re-arranging the terms in the last inequality yields (3.5).

We now turn to (3.6). Using again the triangle inequality together with (3.4) and $\theta_p \leq 1$ yields

$$\begin{aligned} \|g_k\| &\leq \|\nabla\phi(x_k) - g_k\| + \|\nabla\phi(x_k)\| \\ &\leq \max \left\{ \epsilon_g, \sigma_\phi \theta_p \min \left\{ \|\nabla\phi(x_k)\|, \|\nabla\phi(x_k)\| \frac{1+p}{2} \right\} \right\} + \|\nabla\phi(x_k)\| \\ &\leq \sigma_\phi \theta_p \min \left\{ \|\nabla\phi(x_k)\|, \|\nabla\phi(x_k)\| \frac{1+p}{2} \right\} + \|\nabla\phi(x_k)\| \\ &\leq \sigma_\phi \min \left\{ \|\nabla\phi(x_k)\|, \|\nabla\phi(x_k)\| \frac{1+p}{2} \right\} + \|\nabla\phi(x_k)\| \end{aligned} \quad (3.8)$$

$$\leq (1 + \sigma_\phi) \|\nabla\phi(x_k)\|, \quad (3.9)$$

and thus (3.6) holds. \square

To establish a complexity result for our algorithmic framework we divide the iterations into two categories, identified by the indices

$$\begin{aligned} \mathcal{R} &= \{k \in \mathbb{N} \mid d_k = -g_k\} \\ \mathcal{N} &= \mathbb{N} \setminus \mathcal{R}. \end{aligned} \quad (3.10)$$

Any $k \in \mathcal{R}$ is the index of a *restarted iteration*, while $k \in \mathcal{N}$ is the index of a *non-restarted iteration*. Depending on the nature of each iteration, we can bound the number of backtracking steps needed to compute a suitable step size. We begin with the non-restarted iterations, as the proof encompasses that of restarted iterations.

Lemma 3.2 *Let Assumptions 3.1, 3.3, and 3.4 hold. Suppose that the k th iteration of Algorithm 1 is a non-restarted iteration (i.e., $k \in \mathcal{N}$), and that*

$$\min \left\{ \|\nabla\phi(x_k)\|, \|\nabla\phi(x_k)\| \frac{1+p}{2} \right\} \geq \frac{\epsilon_g}{\sigma_\phi \theta_p}, \quad (3.11)$$

where θ_p is defined in (3.2). Then, the line search process terminates after at most $\lceil \bar{j}_{\mathcal{N}} + 1 \rceil$ iterations, where

$$\bar{j}_{\mathcal{N}} := \lceil \log_{\rho}(\theta_p) \rceil_+ \quad (3.12)$$

and $\lceil t \rceil_+ = \max\{t, 0\}$. Moreover, the resulting decrease at the k th iteration satisfies

$$\phi(x_k) - \phi(x_{k+1}) > c_{\mathcal{N}} \epsilon_{\mathbf{g}}^{1+p} - 4\epsilon_f \quad (3.13)$$

where

$$c_{\mathcal{N}} := \eta \sigma_{\mathbf{d}} \frac{(1 - \sigma_{\phi})^{1+p}}{\sigma_{\phi}^{1+p} \theta_p^{1+p}} \min\{1, \rho \hat{\alpha}_p\}, \quad \text{and} \quad \hat{\alpha}_p := \frac{(1 - \eta) \sigma_{\mathbf{d}} (1 - \sigma_{\phi})^{1+p}}{L \kappa_{\mathbf{d}}^2 (1 + \sigma_{\phi})^{1+p}}.$$

Proof. Suppose first that $\alpha_k = 1$ satisfies the Armijo-type condition. In that case, (3.12) holds, and condition (2.3) together with $k \in \mathcal{N}$ gives

$$f(x_k) - f(x_{k+1}) > -\eta g_k^{\mathbf{T}} d_k - 2\epsilon_f > \eta \sigma_{\mathbf{d}} \|g_k\|^{1+p} - 2\epsilon_f. \quad (3.14)$$

Combining Assumption 3.3, (3.5), (3.11) and (3.14) together with the fact that $\sigma_{\phi} \theta_p \leq 1$, it follows that

$$\begin{aligned} \phi(x_k) - \phi(x_{k+1}) &\geq f(x_k) - f(x_{k+1}) - 2\epsilon_f \\ &\geq \eta \sigma_{\mathbf{d}} \|g_k\|^{1+p} - 4\epsilon_f \\ &\geq \eta \sigma_{\mathbf{d}} (1 - \sigma_{\phi})^{1+p} \|\nabla \phi(x_k)\|^{1+p} - 4\epsilon_f \\ &\geq \eta \sigma_{\mathbf{d}} (1 - \sigma_{\phi})^{1+p} \left[\frac{\epsilon_{\mathbf{g}}}{\sigma_{\phi} \theta_p} \right]^{1+p} - 4\epsilon_f \\ &\geq c_{\mathcal{N}} \epsilon_{\mathbf{g}}^{1+p} - 4\epsilon_f. \end{aligned}$$

As a result, (3.13) holds in that case.

Suppose now that the line search condition fails for some $\alpha = \rho^j$ with $j \in \mathbb{N}$, i.e., (2.3) does not hold,

$$\eta \alpha g_k^{\mathbf{T}} d_k \leq f(x_k + \alpha d_k) - f(x_k) - 2\epsilon_f$$

By Assumption 3.1 and (3.1), it follows that

$$\begin{aligned} \eta \alpha g_k^{\mathbf{T}} d_k &\leq f(x_k + \alpha d_k) - f(x_k) - 2\epsilon_f \\ &\leq \phi(x_k + \alpha d_k) - \phi(x_k) \\ &\leq \alpha \nabla \phi(x_k)^{\mathbf{T}} d_k + \frac{L}{2} \alpha^2 \|d_k\|^2. \end{aligned}$$

Subtracting $g_k^{\mathbf{T}} d_k$ from both sides and dividing by α

$$\begin{aligned} -(1 - \eta) g_k^{\mathbf{T}} d_k &\leq [\nabla \phi(x_k) - g_k]^{\mathbf{T}} d_k + \frac{L}{2} \alpha \|d_k\|^2 \\ &\leq \|\nabla \phi(x_k) - g_k\| \|d_k\| + \frac{L}{2} \alpha \|d_k\|^2. \end{aligned}$$

Since $k \in \mathcal{N}$, condition (2.5) is satisfied. Using both inequalities in (2.5), it follows that the above inequality can be bounded as follows

$$(1 - \eta) \sigma_{\mathbf{d}} \|g_k\|^{1+p} \leq \kappa_{\mathbf{d}} \|\nabla \phi(x_k) - g_k\| \|g_k\|^{\frac{1+p}{2}} + \frac{L \kappa_{\mathbf{d}}^2}{2} \alpha \|g_k\|^{(1+p)}.$$

By (3.2) and (3.11),

$$\begin{aligned} (1 - \eta)\sigma_d \|g_k\|^{1+p} &\leq \kappa_d \sigma_\phi \theta_p \min \left\{ \|\nabla\phi(x_k)\|, \|\nabla\phi(x_k)\|^{\frac{1+p}{2}} \right\} \|g_k\|^{\frac{1+p}{2}} + \frac{L\kappa_d^2}{2} \alpha \|g_k\|^{1+p} \\ &\leq \kappa_d \sigma_\phi \theta_p \|\nabla\phi(x_k)\|^{\frac{1+p}{2}} \|g_k\|^{\frac{1+p}{2}} + \frac{L\kappa_d^2}{2} \alpha \|g_k\|^{1+p}. \end{aligned}$$

Using Lemma 3.1 to bound the $\|g_k\|$ terms yields

$$\begin{aligned} &(1 - \eta)\sigma_d (1 - \sigma_\phi)^{1+p} \|\nabla\phi(x_k)\|^{1+p} \\ &\leq \kappa_d \sigma_\phi (1 + \sigma_\phi)^{\frac{1+p}{2}} \theta_p \|\nabla\phi(x_k)\|^{1+p} + \frac{L\kappa_d^2 (1 + \sigma_\phi)^{1+p}}{2} \alpha \|\nabla\phi(x_k)\|^{1+p}. \end{aligned} \quad (3.15)$$

By the definition of θ_p and $\sigma_\phi \leq 1$, we have

$$\kappa_d \sigma_\phi (1 + \sigma_\phi)^{\frac{1+p}{2}} \theta_p \|\nabla\phi(x_k)\|^{1+p} \leq \frac{1}{2} (1 - \eta)\sigma_d (1 - \sigma_\phi)^{1+p} \|\nabla\phi(x_k)\|^{1+p},$$

and thus,

$$\frac{(1 - \eta)\sigma_d (1 - \sigma_\phi)^{1+p}}{2} \|\nabla\phi(x_k)\|^{1+p} \leq \frac{L\kappa_d^2 (1 + \sigma_\phi)^{1+p}}{2} \alpha \|\nabla\phi(x_k)\|^{1+p}.$$

Since $\|\nabla\phi(x_k)\| > 0$ by (3.11), this inequality can be further rewritten as

$$\alpha \geq \frac{(1 - \eta)\sigma_d (1 - \sigma_\phi)^{1+p}}{L\kappa_d^2 (1 + \sigma_\phi)^{1+p}} = \hat{\alpha}_p.$$

Overall, we have shown that if the decrease condition (2.3) fails for a step size α , then

$$\alpha \geq \hat{\alpha}_p. \quad (3.16)$$

The condition (3.16) can only hold if $j \leq \bar{j}_\mathcal{N}$, and thus the backtracking process must terminate after $j_k \leq \lceil \bar{j}_\mathcal{N} \rceil$ iterations. In addition, since this process did not terminate with $\alpha = \rho^{j_k-1}$, it must be that

$$\rho^{j_k-1} \geq \hat{\alpha}_p,$$

hence, $\alpha_k = \rho^{j_k} \geq \rho \hat{\alpha}_p$. By the line search condition (2.3), the fact that $k \in \mathcal{N}$ and (3.11),

$$\begin{aligned} \phi(x_k) - \phi(x_{k+1}) &\geq f(x_k) - f(x_{k+1}) - 2\epsilon_f \\ &\geq -\eta \alpha_k g_k^\top d_k - 4\epsilon_f \\ &\geq \eta \rho \hat{\alpha}_p \sigma_d \|g_k\|^{1+p} - 4\epsilon_f \\ &\geq \eta \rho \hat{\alpha}_p \sigma_d (1 - \sigma_\phi)^{1+p} \|\nabla\phi(x_k)\|^{1+p} - 4\epsilon_f \\ &\geq \eta \rho \hat{\alpha}_p \sigma_d (1 - \sigma_\phi)^{1+p} \left[\frac{\epsilon_g}{\sigma_\phi \theta_p} \right]^{1+p} - 4\epsilon_f \\ &\geq c_{\mathcal{N}} \epsilon_g^{1+p} - 4\epsilon_f, \end{aligned}$$

and hence (3.13) also holds in the latter case. Combining both cases finally yields the desired result. \square

We now consider the restarted iterations, i.e., $k \in \mathcal{R}$. In this case, we have $d_k = -g_k$.

Lemma 3.3 *Let Assumptions 3.1, 3.3 and 3.4 hold. Suppose that the k th iteration of Algorithm 1 is a restarted iteration (i.e., $k \in \mathcal{R}$), and that*

$$\|\nabla\phi(x_k)\| \geq \frac{\epsilon_g}{\sigma_\phi\theta_1}, \quad \text{where} \quad \theta_1 = \frac{(1-\eta)(1-\sigma_\phi)^2}{2(1+\sigma_\phi)}. \quad (3.17)$$

Then, the line search process terminates after at most $\lceil \bar{j}_{\mathcal{R}} + 1 \rceil$ iterations, where

$$\bar{j}_{\mathcal{R}} := \lceil \log_\rho(\theta_1) \rceil_+. \quad (3.18)$$

Moreover, the resulting decrease at the k th iteration satisfies

$$\phi(x_k) - \phi(x_{k+1}) > c_{\mathcal{R}}\epsilon_g^2 - 4\epsilon_f \quad (3.19)$$

where

$$c_{\mathcal{R}} := \eta \frac{(1-\sigma_\phi)^2}{\sigma_\phi^2\theta_1^2} \min\{1, \rho\hat{\alpha}_1\} \quad \text{and} \quad \hat{\alpha}_1 := \frac{(1-\eta)(1-\sigma_\phi)^2}{L(1+\sigma_\phi)^2}.$$

Proof. The proof is a mere restatement of that of Lemma 3.2 with special values for the parameters. Indeed, at every restarted iteration, condition (2.5) holds with

$$\sigma_d = 1, \quad \kappa_d = 1, \quad p = 1,$$

so that $\theta_p = \theta_1$. The rest of the proof follows. \square

The results of Lemmas 3.2 and 3.3 are instrumental to bounding the number of iterations necessary to reach an approximate stationary point.

3.2 Main results

Our main result is a bound on the number of iterations required by the algorithm prior to reaching an approximate stationary point (2.2). This bound also applies to the number of objective function gradient evaluations.

Theorem 3.1 *Let Assumptions 3.1 and 3.2 hold. Suppose further that Assumptions 3.3 and 3.4 hold with*

$$\epsilon_f \leq \min \left[\frac{c_{\mathcal{N}}}{8} \epsilon_g^{1+p}, \frac{c_{\mathcal{R}}}{8} \epsilon_g^2 \right] \quad (3.20)$$

and let

$$\epsilon := \max \left\{ \frac{\epsilon_g}{\sigma_\phi\theta_p}, \left[\frac{\epsilon_g}{\sigma_\phi\theta_p} \right]^{\frac{2}{1+p}}, \frac{\epsilon_g}{\sigma_\phi\theta_1} \right\}.$$

Then, the number of iterations (and gradient estimates) required by Algorithm 1 to reach a point satisfying (2.2) is at most

$$K_\epsilon := \left\lceil \frac{2(\phi(x_0) - \phi_{\text{low}})}{c_{\mathcal{R}}} \epsilon_g^{-2} + \frac{2(\phi(x_0) - \phi_{\text{low}})}{c_{\mathcal{N}}} \epsilon_g^{-(1+p)} \right\rceil. \quad (3.21)$$

Proof. Let $K \in N$ be such that $\|\nabla\phi(x_k)\| > \epsilon$ for any $k = 0, \dots, K-1$. Following our partitioning (3.10), we define the index sets

$$\begin{aligned}\mathcal{N}_K &:= \mathcal{N} \cap \{0, \dots, K-1\}, \\ \mathcal{R}_K &:= \mathcal{R} \cap \{0, \dots, K-1\}.\end{aligned}$$

For any $k \in \mathcal{N}_K$, the result of Lemma 3.2 applies, and we have

$$\phi(x_k) - \phi(x_{k+1}) > c_{\mathcal{N}}\epsilon_g^{1+p} - 4\epsilon_f \geq \frac{c_{\mathcal{N}}}{2}\epsilon_g^{1+p}. \quad (3.22)$$

On the other hand, if $k \in \mathcal{R}_K$, applying Lemma 3.3 gives

$$\phi(x_k) - \phi(x_{k+1}) > c_{\mathcal{R}}\epsilon_g^2 - 4\epsilon_f \geq \frac{c_{\mathcal{R}}}{2}\epsilon_g^2. \quad (3.23)$$

We now consider the sum of function changes over all $k \in \{0, \dots, K-1\}$. By Assumption 3.2, we obtain

$$\begin{aligned}\phi(x_0) - \phi_{\text{low}} &\geq \phi(x_0) - \phi(x_K) \\ &\geq \sum_{k=0}^{K-1} [\phi(x_k) - \phi(x_{k+1})] \\ &\geq \sum_{k \in \mathcal{N}_K} [\phi(x_k) - \phi(x_{k+1})] + \sum_{k \in \mathcal{R}_K} [\phi(x_k) - \phi(x_{k+1})] \\ &> \sum_{k \in \mathcal{N}_K} \frac{c_{\mathcal{N}}}{2}\epsilon_g^{1+p} + \sum_{k \in \mathcal{R}_K} \frac{c_{\mathcal{R}}}{2}\epsilon_g^2.\end{aligned}$$

Since the right-hand side consists of two sums of positive terms, the above inequality implies that

$$\phi(x_0) - \phi_{\text{low}} > \sum_{k \in \mathcal{N}_K} \frac{c_{\mathcal{N}}}{2}\epsilon_g^{1+p} \Leftrightarrow |\mathcal{N}_K| < \frac{2(\phi(x_0) - \phi_{\text{low}})}{c_{\mathcal{N}}}\epsilon_g^{-(1+p)}$$

and

$$\phi(x_0) - \phi_{\text{low}} > \sum_{k \in \mathcal{R}_K} \frac{c_{\mathcal{R}}}{2}\epsilon_g^2 \Leftrightarrow |\mathcal{R}_K| < \frac{2(\phi(x_0) - \phi_{\text{low}})}{c_{\mathcal{R}}}\epsilon_g^{-2}.$$

Using $|\mathcal{N}_K| + |\mathcal{R}_K| = K$ finally yields

$$K < \frac{2(\phi(x_0) - \phi_{\text{low}})}{c_{\mathcal{R}}}\epsilon_g^{-2} + \frac{2(\phi(x_0) - \phi_{\text{low}})}{c_{\mathcal{N}}}\epsilon_g^{-(1+p)},$$

hence $K \leq K_\epsilon$. \square

By combining the result of Theorem 3.1 with that of Lemmas 3.2 and 3.3, we can also provide an evaluation complexity bound of Algorithm 1.

Corollary 3.1 *Under the assumptions of Theorem 3.1, the number of function evaluations required by Algorithm 1 to reach a point satisfying (2.2) is at most*

$$\left(\lceil \log_\rho(\min\{\theta_p, \theta_1\}) \rceil_+ + 1 \right) K_\epsilon, \quad (3.24)$$

where K_ϵ is defined in (3.21).

Proof. By Lemmas 3.2 and 3.3, any iteration requires at most

$$\max\{\bar{j}_{\mathcal{N}}, \bar{j}_{\mathcal{R}}\} + 1 = \lceil \log_p(\min\{\theta_p, \theta_1\}) \rceil_+ + 1$$

function evaluations. Combining this number with the result of Theorem 3.1 completes the proof. \square

Remark 3.1 *When $p = 1$, our results resemble the results in [3]. When $\epsilon_f = \epsilon_g = \sigma_\phi = 0$, our results match the results obtained by Chan–Renous–Legoubin and Royer for the restarted nonlinear conjugate gradient method [12].*

4 Numerical experiments

In this section, we investigate the numerical behavior of several methods that fit into the line search algorithmic framework with restart conditions and estimates given in Algorithm 1. We evaluate the performance of all methods on a subset of the unconstrained optimization problems from the CUTEst collection [17] in both the noise-free and noisy settings. The purpose of these experiments is threefold: (1) to highlight the merits and limitations of different methods; (2) to understand the effect of the restart conditions; and, (3) to explore the influence of the noise.

4.1 Setup

We implemented our algorithmic framework and different instances of the methods in MATLAB R2024a. Experiments were run on the Longleaf cluster², a Linux-based computing system that contains over 1840 CPU cores across 230 blade servers.

Test problems Our test set consists of 234 unconstrained problems from the CUTEst collection [17] with dimensions between 1 and 1000. We used the new MATLAB implementation and interface of the CUTEst problems developed by Gratton and Toint [18], and the default initial points provided for those problems. We scaled each problem by $\max\{1, \|\nabla\phi_0\|_\infty\}$, where $\nabla\phi_0$ is the true gradient at the initial point.

We considered both noise-free (deterministic) and noisy versions of all the problems. For each problem in the test set, we considered 5 noise levels (including the noise-free setting), namely $\epsilon_f = \{0, 10^{-8}, 10^{-4}, 10^{-2}, 10^{-1}\}$, and $\epsilon_g = \sqrt{\epsilon_f}$. We added uniform noise to the function and gradient evaluations bounded by ϵ_f and ϵ_g , respectively, and assumed that ϵ_f was available to all methods.

Algorithms We compared the following methods.

- (1) **Gradient descent (GD):** Algorithm 1 with $d_k = -g_k$, $p = 1$ and $\kappa_d = \sigma_d^{-1} = 1$.
- (2) **Nonlinear conjugate gradient (NLCG):** Algorithm 1 with $d_k = -g_k + \beta_k d_{k-1}$, where β_k is updated using the PRP+ formula [22] and $\sigma_d = 0$ and $\kappa_d = \infty$.

²<https://help.rc.unc.edu/longleaf-cluster/>

- (3) **Limited-Memory BFGS (LBFGS)**: The classical LBFGS method [27, equation (7.15)]. Algorithm 1 with $d_k = -H_k g_k$, where H_k is updated using the BFGS methodology [27, equation (7.19)] and d_k is computed using the LBFGS two-loop recursion [27, Algorithm 7.4], and $\sigma_d = 0$ and $\kappa_d = \infty$. We consider a memory size $m = 10$, and, as is standard practice, curvature pairs $s_k = x_{k+1} - x_k$ and $y_k = g_{k+1} - g_k$ are only stored if $s_k^T y_k \geq \epsilon_{sy} \|s_k\| \|y_k\|$, where $\epsilon_{sy} = 10^{-4}$ [27].
- (4) **Nonlinear conjugate gradient with restarts (NLGr)**: Algorithm 1 with $d_k = -g_k + \beta_k d_{k-1}$, where β_k is updated using the PRP+ formula [22]. We choose $\kappa_d \in (0, \infty)$ and set $\sigma_d = \kappa_d^{-1}$.
- (5) **Limited-Memory BFGS with restarts (LBFGSr)**: Algorithm 1 with $d_k = -H_k g_k$, where H_k is updated using the BFGS methodology [27, equation (7.19)] and d_k is computed using the LBFGS two-loop recursion [27, Algorithm 7.4]. We consider a memory size $m = 10$, and a similar strategy as that of LBFGS is used to store curvature pairs at every iteration. We choose $\kappa_d \in (0, \infty)$ and set $\sigma_d = \kappa_d^{-1}$.

For methods (2) and (3), the values of $\sigma_d = 0$ and $\kappa_d = \infty$ ensure that the methods only restart if the computed direction is not a descent direction, i.e., if $g_k^T d_k \geq 0$. This, of course, never occurs for method (3). For the restarted variants (4) and (5), we consider multiple values for p and κ_d for a sensitivity analysis, using $\sigma_d = \kappa_d^{-1}$ to restrict this analysis to two parameters. Following the previous study on restarted nonlinear conjugate gradient and line search techniques [8], we set the line search parameters to $\eta = 1/2$ and $\rho = 1/2$. We also consider the PRP+ update rule for β_k since it has proven to be robust and competitive in practice [12]. Finally, all methods were run 10 times on each problem and noise instance to account for randomness in function/gradient estimates.

Termination condition Algorithms were terminated when a maximum number of 1000 iterations was reached, or when $\|g_k\|_\infty \leq \max\{2\epsilon_g, 10^{-8}\}$. Note that this condition implies that wrong termination can occur whenever the noise induces a gradient estimate with small norm. We have encountered this situation at the initial point for 2.6% of the noisy runs, and 5.6% of the runs for the largest noise level. The results presented thereafter discard those runs, and consider a problem to be solved whenever the method computed an iterate $x_{\hat{k}}$ such that

$$\|\nabla\phi(x_{\hat{k}})\|_\infty \leq \epsilon_g + \max\{2\epsilon_g, 10^{-8}\}.$$

This criterion is based on (3.2), and reduces to $\|\nabla\phi(x_{\hat{k}})\|_\infty \leq 10^{-8}$ in the absence of noise.

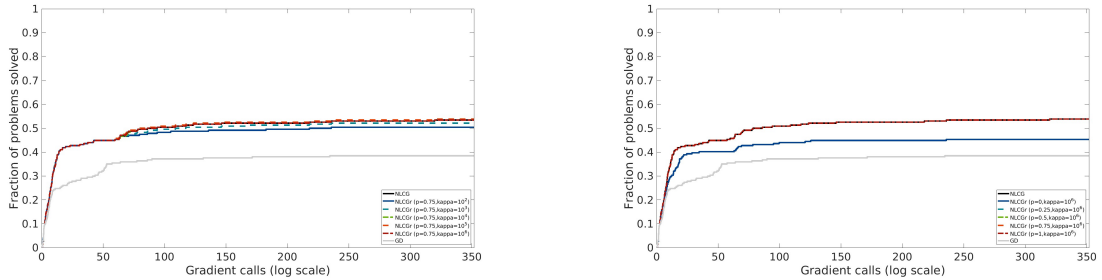
Performance and Data Profiles We compare restarted variants of NLGr and LBFGSr with their non-restarted counterparts as well as gradient descent for several noise levels. We summarize our findings using performance and data profiles [14, 26]. We built performance and data profiles for our tests based on the number of gradient calls (equivalent to the number of iterations) required to achieve a desired tolerance.

4.2 Results in the noiseless setting

We begin our study by investigating the noiseless setting. To this end, and similarly to previous work on restarting NLGr [12], we first compute the average percentage of restarts for all variants for different choices of p and κ_d (per our settings, all restarted variants use $\sigma_d = \kappa_d^{-1}$).

NLCGr						LBFGSr					
$p \backslash \kappa_d$	10^2	10^3	10^4	10^5	10^6	$p \backslash \kappa_d$	10^2	10^3	10^4	10^5	10^6
0	77.86	66.66	54.42	40.84	26.29	0	91.38	81.58	69.21	46.90	21.82
0.25	68.09	52.38	34.43	14.66	0.95	0.25	84.28	62.23	33.16	18.28	11.21
0.50	48.15	21.51	0.92	0.35	0.32	0.50	62.11	32.50	19.84	13.03	6.87
0.75	2.01	0.60	0.40	0.34	0.32	0.75	51.43	28.95	19.50	11.24	6.67
1	2.20	0.70	0.42	0.34	0.32	1	55.84	33.06	19.90	12.55	7.74

Table 1: Percentage of restarted iterations in the noiseless case (Left: NLCGr; Right: LBFGSr).



(a) $p = 0.75$ (the curves for $\kappa \geq 10^4$ overlap with the NLCGr curve).

(b) $\kappa = 10^6$ (the curves for $p \geq 0.25$ overlap with the NLCGr curve).

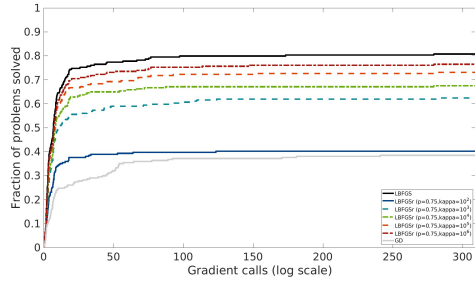
Figure 1: Sensitivity of the performance of restarted nonlinear conjugate gradient (NLCGr) in absence of noise (Data profiles).

Table 1 illustrates that higher values of κ_d (and thus smaller values of σ_d) lead to fewer restarts, i.e., to algorithmic behavior closer to that of the non-restarted variants. A similar observation applies when increasing the value of p . Note, however, that this trend is more pronounced for the NLCGr variants than for the LBFGSr variants. To further highlight the impact of the restarting condition, we compare restarted variants using $p = 0.75$ (with variable κ_d) and $\kappa_d = 10^6$ (with variable p). Figure 1 shows that the performance of restarted NLCGr is quite close to that of standard NLCGr except for the lowest values of p and κ_d . On the other hand, as shown by Figure 2, the choice of p and κ_d has a significant impact on the performance of LBFGSr, with the lowest values leading to a significant number of restarts and thus, performance close to that of gradient descent. Overall, these figures suggest that limiting the number of restarts leads to improved performance, closer to that of the original method.

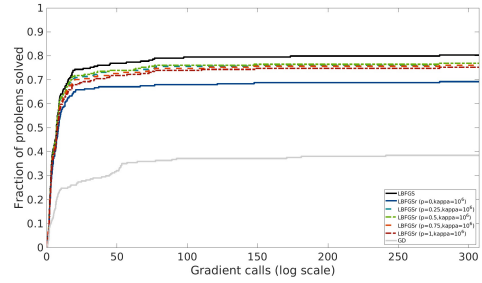
We thus compare GD, classical NLCGr and LBFGSr with NLCGr and LBFGSr using ($p = 0.75, \kappa = 10^6$). Figure 3 shows that the two NLCGr variants perform identically, whereas the performance of LBFGSr is slightly below that of LBFGS. These results confirm the findings of Chan–Renous-Legoubin and Royer in the case of NLCGr [12], while shedding a new light on the use of the restarting condition for LBFGS in the absence of noise.

4.3 Results in noisy settings

In the noisy setting, our experiments reveal a higher variability in the number of restarts for both NLCGr and LBFGSr. Due to the randomized nature of the problems, we now define the best values for p (resp., κ_d) according to the best performance across all possible choices for κ_d

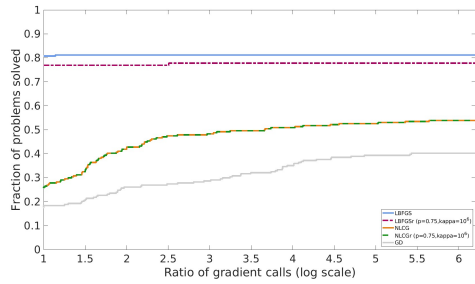


(a) $p = 0.75$.

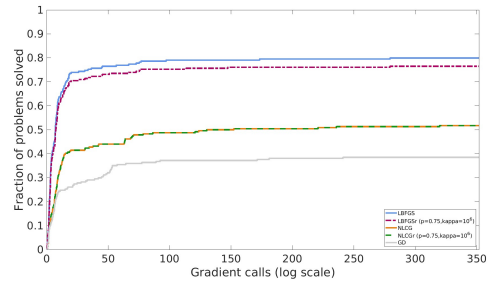


(b) $\kappa = 10^6$.

Figure 2: Sensitivity of the performance of restarted LBFGr (LBFGrS) in absence of noise (Data profiles).



(a) Performance profile.

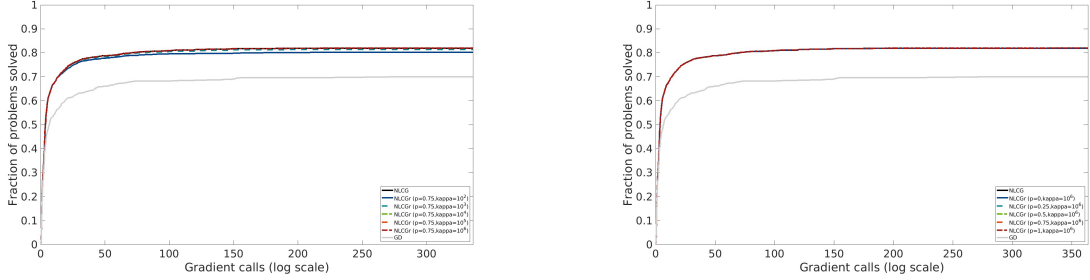


(b) Data profile.

Figure 3: Non-restarted vs. best restarted methods in the absence of noise.

Method	$\epsilon_f = 10^{-8}$	$\epsilon_f = 10^{-4}$	$\epsilon_f = 10^{-2}$	$\epsilon_f = 10^{-1}$
NLCGr	(0.75, 10^6)	(0.75, 10^5)	(0, 10^3)	(0.25, 10^3)
LBFGr	(0.75, 10^6)	(1, 10^6)	(0.5, 10^6)	(0, 10^6)

Table 2: Values of p and κ_d with the least percentage of restarted iterations.



(a) $p = 0.75$ (the curves for $\kappa \geq 10^3$ overlap with the NLCG curve).

(b) $\kappa = 10^6$ (all NLCG curves overlap with the NLCG curve).

Figure 4: Sensitivity of the performance of restarted nonlinear conjugate gradient (NLCGr) with $\epsilon_f = 10^{-8}$ (Data profiles).

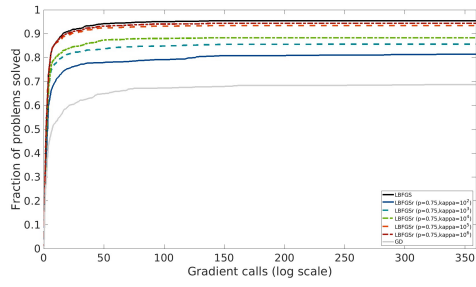
(resp., p). Note that our stopping criterion is less stringent than in the noiseless setting.

Detailed statistics regarding restarts are given in Appendix A, and Table 2 summarizes the best configurations in terms of p and κ_d (recall that we set $\sigma_d = \kappa_d^{-1}$). For LBFGr, using a large value of κ_d is critical, which we attribute to the directions being of relatively high norm compared to that of the gradient. Lower values of p appear preferable as the noise increases. For NLCGr, both the best value of κ_d and that of p decrease as the noise increases. Note these observations are consistent with our analysis, in that the selected values lead to better complexity bounds.

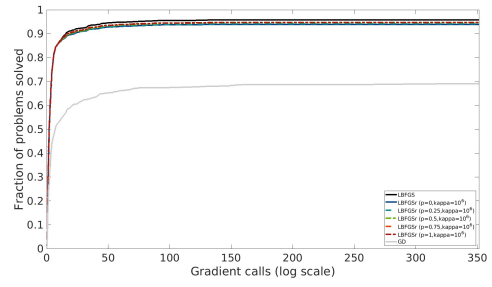
To further motivate these parameter choices, we conducted a sensitivity analysis for the lowest and highest noise levels. When the noise level is relatively low, Figures 4 and 5 yield the same conclusions as in the noiseless case. Indeed, the NLCGr variants coincide with NLCG for sufficiently high values of the parameters. A similar conclusion holds for LBFGr, although we notice that all variants are much closer than in the noiseless case, which we attribute to the lower number of overall restarts performed by those variants (see Table 3, Appendix A for detailed statistics).

For the higher noise level (Figures 6 and 7), we notice that the curves are much closer to one another, for both NLCG and LBFGr. This behavior is largely explained by the convergence criterion used in that case. Indeed, only a low precision on the gradient is required, which all methods manage to satisfy rather easily. The number of restarts is also quite similar for all NLCGr variants, with more variability for LBFGr variants (see Table 6, Appendix A for detailed statistics). Overall, our experiments suggest that using a restarted variant in the presence of noise will lead to performance comparable to that of a non-restarted variant.

To further confirm this observation, we compare GD, NLCG, LBFGr and the two best restarted variants according to Table 2 for all noise levels. Figures 8 to 11 show performance

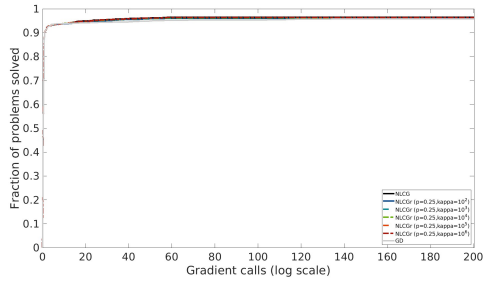


(a) $p = 0.75$.

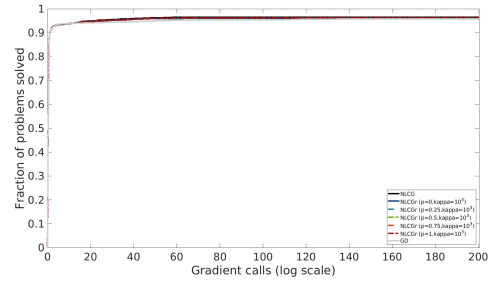


(b) $\kappa = 10^6$ (the curves $p \in \{0.25, 0.5\}$ and $p \in \{0.75, 1\}$ respectively overlap).

Figure 5: Sensitivity of the performance of restarted LBFGS (LBFGSr) with $\epsilon_f = 10^{-8}$ (Data profiles).

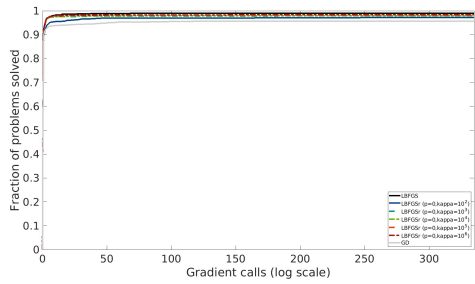


(a) $p = 0.25$.

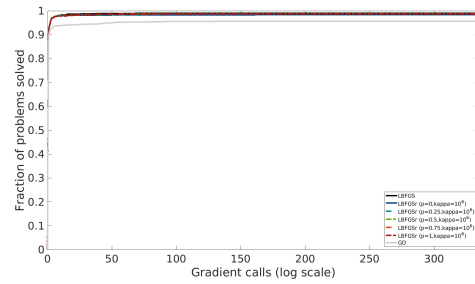


(b) $\kappa = 10^3$.

Figure 6: Sensitivity of the performance of restarted nonlinear conjugate gradient with $\epsilon_f = 10^{-1}$ (Data profiles).



(a) $p = 0$.



(b) $\kappa = 10^6$.

Figure 7: Sensitivity of the performance of restarted LBFGS (LBFGSr) with $\epsilon_f = 10^{-1}$ (Data profiles).

and data profiles for four noise levels. Restarted variants are typically overlapping with their non-restarted counterparts, as in the noiseless case. As the noise increases, we notice that all curves get closer to one another. In particular, gradient descent matches the performance of NLCG variants for $\epsilon_f \geq 10^{-2}$, and the difference between the LBFGS variants and others gets less pronounced as the noise increases. Still, we note that the LBFGS variants exhibit the best performance overall, confirming the interest of such approaches even in noisy settings.

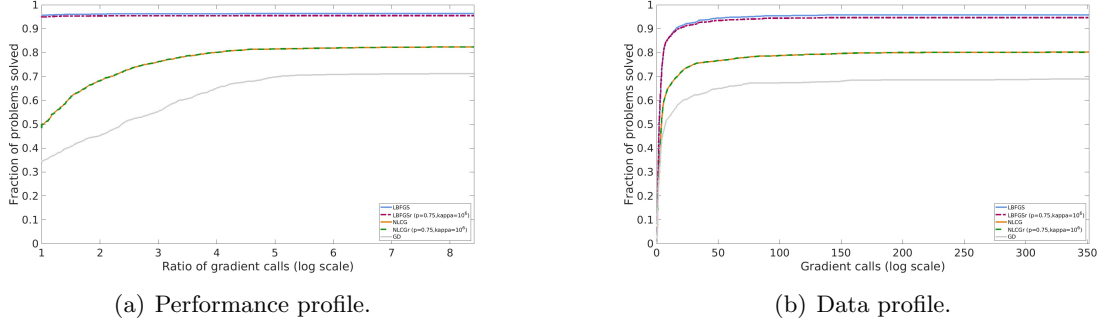


Figure 8: Non-restarted vs. best restarted methods with $\epsilon_f = 10^{-8}$.

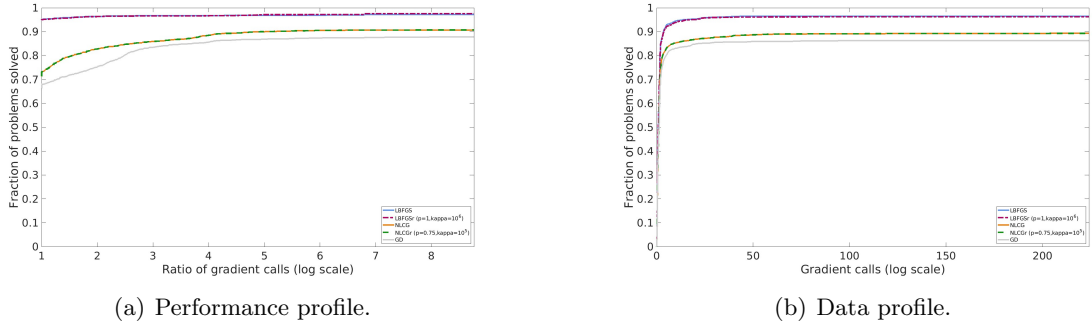


Figure 9: Non-restarted vs. best restarted methods with $\epsilon_f = 10^{-4}$.

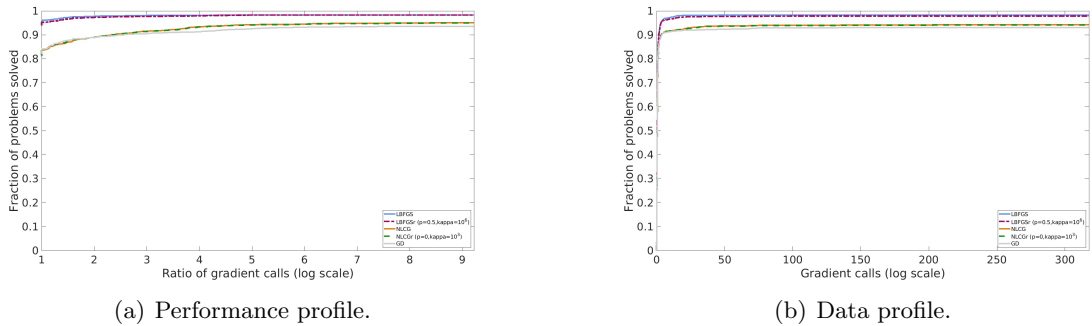


Figure 10: Non-restarted vs. best restarted methods with $\epsilon_f = 10^{-2}$.

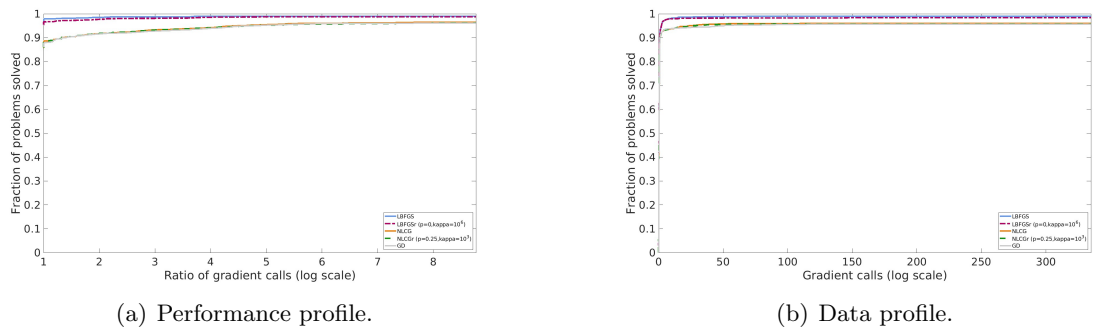


Figure 11: Non-restarted vs. best restarted methods with $\epsilon_f = 10^{-1}$.

5 Conclusion

We have proposed a line search framework for noisy optimization problems in which advanced search direction techniques revert to (inexact) gradient steps when a restarting condition is triggered. These conditions are instrumental to obtaining complexity guarantees, and our analysis highlights that the percentage of restarted iterations has an impact on complexity bounds. The proportion of restarted iterations is also a major factor in the numerical performance. In particular, the performance of LBFSS variants is highly sensitive to the restart condition parameters. When calibrated appropriately, however, a restarted LBFSS method can be competitive with its non-restarted counterpart in both noiseless and noisy settings. NLCG variants are less sensitive to the use of a restarting condition, but perform less favorably in a noisy setting.

Our analysis assumes that our gradient and function estimates satisfy deterministic accuracy conditions. Extending our approach to probabilistic accuracy properties, based on the notion of oracles [3], represents a promising avenue for future research. Investigating other line search techniques would also allow to hew closer to state-of-the-art LBFSS and NLCG techniques.

Acknowledgments We thank the coordinating editor and two anonymous reviewers for their feedback. In particular, we are grateful to one reviewer for pointing out the possibility of choosing θ_p independently of the Lipschitz constant.

Support for this research was partially provided by Agence Nationale de la Recherche through program ANR-19-P3IA-0001 (PRAIRIE 3IA Institute), by the FACE Foundation under the Thomas Jefferson Fund project “Adaptive, Local and Innovative Algorithms for Stochastic Optimization (ALIAS)”, and by the Office of Naval Research under award N00014-24-1-2638.

References

- [1] C. Audet and W. Hare. *Derivative-Free and Blackbox Optimization*. Springer Series in Operations Research and Financial Engineering. Springer International Publishing, 2017.
- [2] A. S. Berahas, R. H. Byrd, and J. Nocedal. Derivative-free optimization of noisy functions via quasi-newton methods. *SIAM J. Optim.*, 29:965–993, 2019.

- [3] A. S. Berahas, L. Cao, and K. Scheinberg. Global convergence rate analysis of a generic line search algorithm with noise. *SIAM J. Optim.*, 31:1489–1518, 2021.
- [4] E. Berglund, J. Zhang, and M. Johansson. Soft quasi-Newton: guaranteed positive definiteness by relaxing the secant constraint. *Optim. Methods Softw.*, 40:783–812, 2025.
- [5] L. Bottou, F. E. Curtis, and J. Nocedal. Optimization Methods for Large-Scale Machine Learning. *SIAM Rev.*, 60:223–311, 2018.
- [6] R. H. Byrd, G. M. Chin, J. Nocedal, and Y. Wu. Sample size selection in optimization methods for machine learning. *Math. Program.*, 134:127–155, 2012.
- [7] L. Cao, A. S. Berahas, and K. Scheinberg. First-and second-order high probability complexity bounds for trust-region methods with noisy oracles. *Math. Program.*, 207:55–106, 2024.
- [8] Y. Carmon, J. C. Duchi, O. Hinder, and A. Sidford. “Convex until proven guilty”: Dimension-free acceleration of gradient descent on non-convex functions. In *Proceedings of the International Conference on Machine Learning, August 2017, Sydney, Australia*, pages 654–663, 2017.
- [9] R. G. Carter. On the global convergence of trust region algorithms using inexact gradient information. *SIAM J. Numer. Anal.*, 28:251–265, 1991.
- [10] C. Cartis, Ph. R. Sampaio, and Ph. L. Toint. Worst-case evaluation complexity of non-monotone gradient-related algorithms for unconstrained optimization. *Optimization*, 64:1349–1361, 2015.
- [11] C. Cartis and K. Scheinberg. Global convergence rate analysis of unconstrained optimization methods based on probabilistic models. *Math. Program.*, 169:337–375, 2018.
- [12] R. Chan–Renous-Legoubin and C. W. Royer. A nonlinear conjugate gradient method with complexity guarantees and its application to nonconvex regression. *Euro. J. Comput. Optim.*, 10:100044, 2022.
- [13] A. R. Conn, K. Scheinberg, and L. N. Vicente. *Introduction to derivative-free optimization*. SIAM, 2009.
- [14] E. D. Dolan and J. J. Moré. Benchmarking optimization software with performance profiles. *Math. Program.*, 91:201–213, 2002.
- [15] J. C. Duchi, M. I. Jordan, M. J. Wainwright, and A. Wibisono. Optimal rates for zero-order convex optimization: The power of two function evaluations. *IEEE Transactions on Information Theory*, 61:2788–2806, 2015.
- [16] M. Fazel, R. Ge, S. Kakade, and M. Mesbahi. Global convergence of policy gradient methods for the linear quadratic regulator. In *International Conference on Machine Learning*, pages 1467–1476. PMLR, 2018.
- [17] N. I. M. Gould, D. Orban, and Ph. L. Toint. CUTEst: a constrained and unconstrained testing environment with safe threads. *Comput. Optim. Appl.*, 60:545–557, 2015.

- [18] S. Gratton and Ph. L. Toint. S2MPJ and CUTEst optimization problems for Matlab, Python and Julia. arXiv:2407.07812, 2024.
- [19] L. Grippo and S. Lucidi. Convergence conditions, line search algorithms and trust region implementations for the Polak-Ribière conjugate gradient method. *Optim. Methods Softw.*, 20:71–98, 2005.
- [20] W. W. Hager and H. Zhang. A new conjugate gradient method with guaranteed descent and an efficient line search. *SIAM J. Optim.*, 16:170–192, 2005.
- [21] W. W. Hager and H. Zhang. Algorithm 851: CG_DESCENT, a conjugate gradient method with guaranteed descent. *ACM Trans. Math. Software*, 32:113–137, 2006.
- [22] W. W. Hager and H. Zhang. A survey of nonlinear conjugate gradient methods. *Pac. J. Optim.*, 2:35–58, 2006.
- [23] B. Irwin and E. Haber. Secant penalized BFGS: a noise robust quasi-Newton method via penalizing the secant condition. *Comput. Optim. Appl.*, 84:651–702, 2023.
- [24] B. Jin, K. Scheinberg, and M. Xie. High probability complexity bounds for adaptive step search based on stochastic oracles. *SIAM J. Optim.*, 34:2411–2439, 2024.
- [25] J. Larson, M. Menickelly, and S. M. Wild. Derivative-free optimization methods. *Acta Numerica*, 28:287–404, 2019.
- [26] J.J. Moré and S. M. Wild. Benchmarking derivative-free optimization algorithms. *SIAM J. Optim.*, 20:172–191, 2009.
- [27] J. Nocedal and S. J. Wright. *Numerical Optimization*. Springer Ser. Oper. Res. Financ. Eng. Springer-Verlag, New York, second edition, 2006.
- [28] C. Paquette and K. Scheinberg. A stochastic line search method with convergence rate analysis. *SIAM J. Optim.*, 30:349–376, 2020.
- [29] R. Pasupathy, P. Glynn, S. Ghosh, and F. S. Hashemi. On sampling rates in simulation-based recursions. *SIAM J. Optim.*, 28(1):45–73, 2018.
- [30] S. Shashaani, F. S. Hashemi, and R. Pasupathy. Astro-df: A class of adaptive sampling trust-region algorithms for derivative-free stochastic optimization. *SIAM J. Optim.*, 28(4):3145–3176, 2018.
- [31] H.-J. M. Shi, Y. Xie, R. H. Byrd, and J. Nocedal. A noise-tolerant quasi-Newton algorithm for unconstrained optimization. *SIAM J. Optim.*, 32:29–55, 2022.
- [32] S. Sun and J. Nocedal. A trust region method for noisy unconstrained optimization. *Math. Program.*, 202:445–472, 2023.
- [33] S. J. Wright and B. Recht. *Optimization for Data Analysis*. Cambridge University Press, 2022.
- [34] Y. Xie, R. H. Byrd, and J. Nocedal. Analysis of the BFGS method with errors. *SIAM J. Optim.*, 30:182–209, 2020.

A Full restart statistics in the noisy setting

In Tables 3-6, bold numbers represent the pair (p, κ) corresponding to the lowest percentage of restarts in the corresponding table, and italicized numbers represent the best overall values of p (resp., κ_d) for different values of κ_d (resp., p).

NLCGr						LBFGSr					
$p \backslash \kappa_d$	10^2	10^3	10^4	10^5	10^6	$p \backslash \kappa$	10^2	10^3	10^4	10^5	10^6
0	59.04	23.04	11.28	10.62	<i>10.58</i>	0	46.18	27.77	18.47	13.15	<i>6.13</i>
0.25	31.80	11.10	10.62	10.60	<i>10.58</i>	0.25	35.43	22.17	15.58	9.94	<i>5.18</i>
0.50	11.27	10.40	10.63	10.61	<i>10.60</i>	0.50	32.87	19.07	12.43	7.17	<i>3.81</i>
0.75	<i>10.71</i>	<i>10.48</i>	<i>10.62</i>	<i>10.60</i>	<i>10.60</i>	0.75	<i>34.94</i>	<i>16.99</i>	<i>11.48</i>	<i>4.62</i>	3.54
1	11.07	10.58	10.65	10.61	<i>10.61</i>	1	41.50	17.26	8.68	4.89	<i>3.35</i>

Table 3: Percentage of restarted iterations with $\epsilon_f = 10^{-8}$ (Left: NLCG; Right: LBFGS).

NLCGr						LBFGSr					
$p \backslash \kappa_d$	10^2	10^3	10^4	10^5	10^6	$p \backslash \kappa$	10^2	10^3	10^4	10^5	10^6
0	16.30	14.11	13.81	13.72	13.72	0	26.11	16.63	8.88	5.83	<i>2.74</i>
0.25	14.82	14.05	13.78	13.72	13.77	0.25	23.10	14.93	8.35	5.18	2.52
0.50	14.63	13.99	13.75	<i>13.73</i>	13.82	0.50	21.31	13.37	8.07	4.02	<i>2.53</i>
0.75	<i>14.51</i>	<i>13.95</i>	<i>13.73</i>	<i>13.77</i>	<i>13.89</i>	0.75	20.39	12.32	6.97	3.91	<i>2.59</i>
1	14.53	13.90	13.75	<i>13.86</i>	13.89	1	<i>20.07</i>	<i>11.91</i>	<i>5.83</i>	<i>3.98</i>	<i>2.62</i>

Table 4: Percentage of restarted iterations with $\epsilon_f = 10^{-4}$ (Left: NLCG; Right: LBFGS).

NLCGr						LBFGSr					
$p \backslash \kappa_d$	10^2	10^3	10^4	10^5	10^6	$p \backslash \kappa$	10^2	10^3	10^4	10^5	10^6
0	<i>14.22</i>	<i>13.82</i>	13.71	<i>13.82</i>	<i>13.87</i>	0	17.62	7.56	4.32	1.75	1.18
0.25	14.16	<i>13.74</i>	13.75	13.86	13.94	0.25	16.38	8.22	4.48	1.92	<i>1.34</i>
0.50	14.11	<i>13.72</i>	13.80	13.88	13.95	0.50	<i>15.51</i>	<i>8.37</i>	<i>4.43</i>	<i>2.15</i>	<i>1.57</i>
0.75	14.05	<i>13.74</i>	13.84	13.94	13.94	0.75	15.32	8.48	4.27	2.43	<i>1.71</i>
1	14.01	<i>13.81</i>	13.88	13.95	13.94	1	14.81	8.78	4.45	2.53	<i>1.87</i>

Table 5: Percentage of restarted iterations with $\epsilon_f = 10^{-2}$ (Left: NLCG; Right: LBFGS).

NLCGr						LBFGSr					
$p \setminus \kappa_d$	10^2	10^3	10^4	10^5	10^6	$p \setminus \kappa$	10^2	10^3	10^4	10^5	10^6
0	16.22	<i>15.81</i>	15.83	15.89	15.93	0	<i>9.85</i>	<i>5.02</i>	<i>3.21</i>	<i>1.29</i>	<i>0.89</i>
0.25	<i>16.08</i>	<i>15.80</i>	<i>15.88</i>	<i>15.92</i>	<i>15.92</i>	0.25	10.36	5.68	3.25	1.66	<i>1.07</i>
0.50	16.05	<i>15.83</i>	15.88	15.93	15.92	0.50	11.43	6.64	3.49	1.87	<i>1.39</i>
0.75	16.09	<i>15.83</i>	15.91	15.92	15.92	0.75	11.87	6.90	3.78	2.24	<i>1.50</i>
1	16.08	<i>15.90</i>	15.93	15.93	15.92	1	12.13	7.09	4.20	2.46	<i>1.53</i>

Table 6: Percentage of restarted iterations with $\epsilon_f = 10^{-1}$ (Left: NLCG; Right: LBFGS).